The life cycle of crevasse splays as a key mechanism in the aggradation of alluvial ridges and river avulsion

van Toorenenburg, Koen A.; Donselaar, Marinus E.; Weltje, Gert Jan

DOI
10.1002/esp.4404

Publication date
2018

Document Version
Final published version

Published in
Earth Surface Processes and Landforms

Citation (APA)
van Toorenenburg, K. A., Donselaar, M. E., & Weltje, G. J. (2018). The life cycle of crevasse splays as a key mechanism in the aggradation of alluvial ridges and river avulsion. *Earth Surface Processes and Landforms*, *43*(11), 2409-2420. https://doi.org/10.1002/esp.4404

EARTH SURFACE PROCESSES AND LANDFORMS
Earth Surf. Process. Landforms **43**, 2409–2420 (2018)

Published online 18 May 2018 in Wiley Online Library
(wileyonlinelibrary.com) DOI: 10.1002/esp.4404

The life cycle of crevasse splays as a key mechanism in the aggradation of alluvial ridges and river avulsion

Koen A. van Toorenenburg,[1]* Marinus E. Donselaar[1] and Gert Jan Weltje[2]
[1] Department of Geoscience and Engineering, Delft University of Technology, Delft, The Netherlands
[2] Department of Earth and Environmental Sciences, University of Leuven, Leuven, Belgium

Received 22 September 2017; Revised 5 April 2018; Accepted 16 April 2018

*Correspondence to: Koen van Toorenenburg, Department of Geoscience and Engineering, Delft University of Technology, P.O. Box 5048, 2600 GA Delft, The Netherlands. E-mail: k.a.vantoorenenburg@tudelft.nl

ESPL
Earth Surface Processes and Landforms

ABSTRACT: Accommodation space in the unconfined distal part of low-gradient fluvial fans facilitates abundant floodplain deposition. Here, the development of crevasse splays plays a key role in the aggradation of alluvial ridges and subsequent river avulsion. This study presents an analysis of different stages in the evolution of crevasse splays based on observations made in the modern-day Río Colorado dryland fluvial fan fringing the endorheic Altiplano Basin in Bolivia. A generic life cycle is proposed in which crevasse-splay channels adjust towards a graded equilibrium profile with their lower-lying distal termini acting as a local base level. Initial development is dominantly controlled by the outflow of floodwater, promoting erosion near the crevasse apex and deposition towards the splay fringes. When proximal incision advances to below the maximum level of floodplain inundation, return flow occurs during the waning stage of flooding. This floodwater reflux leads to a temporary repositioning of the local base level to the deeper trunk-channel thalweg at the apex of the crevasse-splay channels. The resultant decrease in the floodplainward gradient of these channels ultimately leads to backfilling and abandonment of the crevasse splay, leaving a subtle local elevation of the floodplain. Consecutive splays form an alluvial ridge through lateral amalgamation and subsequent vertical stacking, which is mirrored by the aggradation of their parent channel floor. As this alluvial ridge becomes increasingly perched above the surrounding floodplain, splay equilibration may cause incision of the levee crevasse down to or below its trunk channel thalweg, leading to an avulsion. The mechanisms proposed in this study are relevant to fluvial settings promoting progradational avulsions. The relatively rapid accumulation rate and high preservation potential of crevasse splays in this setting makes them an important constituent of the resultant fluvial stratigraphy, amongst which are hydrocarbon-bearing successions. Copyright © 2018 John Wiley & Sons, Ltd.

KEYWORDS: crevasse-splay life cycle; alluvial ridges; aggrading fluvial fans; avulsion mechanism; preserved stratigraphy

Introduction

Fluvial research generally focuses on the (near) channel domain, which represents the most dynamic environment in river systems. Sedimentation in the unconfined distal part of low-gradient fluvial fans, however, is dominated by floodplain deposition (e.g. Nichols and Fisher, 2007). Here, floodplain evolution has a significant influence on river dynamics, constituting a dynamic boundary condition for the development of the system. Relative to other depositional floodplain processes (i.e. disregarding vegetation), fluvial levees and crevasse splays represent the highest accumulation rates.

On low-gradient alluvial plains, away from topographic confinement, levees likely grow by advection as a water-surface gradient is established between the channel and the adjacent floodplain when peak discharge results in unconfined overbank flow (Adams *et al.*, 2004; Cahoon *et al.*, 2011). Sediment mobilized by the increased in-channel stream power is redeposited in these broad low-gradient levees, decreasing in grain size with distance from the main channel (Adams *et al.*, 2004). Subsequent floodplain inundation allows finer sediment to precipitate from suspension over a large area (Nicholas and Walling, 1997).

The formation of crevasse splays is conditional upon the presence of levees and initiates from a breach point (e.g. Tooth, 2005). The acute onset of crevassing can be arbitrary and has been attributed to fluvial spillover (e.g. Smith *et al.*, 1998; Li and Bristow, 2015), local depressions or weaknesses in the levee crest (Smith *et al.*, 1998; Slingerland and Smith, 2004; Kleinhans *et al.*, 2013), and downstream narrowing (e.g. Li *et al.*, 2014b) or blockage of the main channel caused by, e.g. bank collapse or obstruction by foreign objects (Keller and Swanson, 1979; Slingerland and Smith, 2004; Bridge, 2006; Bernal *et al.*, 2013). Initially, the overbank gradient and breach-point focusing of floodwater lead to erosion and incision of crevasse-splay channels (Yuill *et al.*, 2016), remobilizing levee sediment and the underlying substrate. Deposition occurs where the flow decelerates due to a transition from confined to unconfined flow (cf. Sheets *et al.*, 2002), a decrease in gradient (cf. Bull, 1979), or the floodwater entering a standing body

of water (Bristow *et al.*, 1999; Pérez-Arlucea and Smith, 1999; Bridge, 2006; Millard *et al.*, 2017). The splay is deposited as a complex of small lobes that amalgamate as crevasse-splay channels switch and bifurcate (Smith *et al.*, 1989; Tooth, 2005). It expands and progrades further onto the floodplain over the course of consecutive flooding events, its size and floodwater capacity dependent on the overbank morphology and crevasse dimensions (Yuill *et al.*, 2016). The aerial extent of crevasse splays may reach up to several square kilometres (Burns *et al.*, 2017), depending primarily on sediment size and floodplain-drainage conditions (Millard *et al.*, 2017). Crevasse splays extend from both sides of the main channel, generally increasing in frequency downstream (Li and Bristow, 2015). Crevasse-splay channels may be reused by return flow of floodwater to their trunk river during the waning stage of flooding, leading to the development of sinuous rill channels where surface runoff enters a channel depression (Zwoliński, 1992; Donselaar *et al.*, 2013). This reflux causes backstepping erosion of the hanging crevasse-splay channel floor at its confluence with the main river and in-channel deposition of sedimentary lobes downstream of the channel junction (Donselaar *et al.*, 2013).

Existing research with a dedicated focus on crevasse splays generally concerns depositional processes and (preserved) sedimentary architecture. These studies are based on observations in modern-day river systems (e.g. Arndorfer, 1973; O'Brien and Wells, 1986; Smith *et al.*, 1989; van Gelder *et al.*, 1994; Bristow *et al.*, 1999; Farrell, 2001; Tooth, 2005; Cahoon *et al.*, 2011; Li and Bristow, 2015; Shen *et al.*, 2015; Joeckel *et al.*, 2016; Millard *et al.*, 2017) and examples of ancient deposits in outcrop (e.g. Platt and Keller, 1992; Mjøs *et al.*, 1993; Hornung and Aigner, 1999; Anderson, 2005; Fisher *et al.*, 2007; Hampton and Horton, 2007; Jones and Hajek, 2007; Nichols and Fisher, 2007; Ghazi and Mountney, 2009; Pranter *et al.*, 2009; Ford and Pyles, 2014; Gulliford *et al.*, 2014; Sahoo *et al.*, 2016; Van Toorenenburg *et al.*, 2016; Burns *et al.*, 2017) or in the subsurface (e.g. Pranter *et al.*, 2008; McKie, 2011b; Keeton *et al.*, 2015). Yuill *et al.* (2016) point out that despite being given minor attention, erosional processes play an important role in the initial phase of crevasse-splay development.

The evolution of crevasse splays is often associated with avulsion of the main river (e.g. Smith *et al.*, 1989; Smith and Pérez-Arlucea, 1994; Bristow *et al.*, 1999; Mohrig *et al.*, 2000; Farrell, 2001; Slingerland and Smith, 2004; Tooth, 2005; Hampton and Horton, 2007; Dalman and Weltje, 2008; Buehler *et al.*, 2011; Hajek and Wolinsky, 2012; Bernal *et al.*, 2013; Kleinhans *et al.*, 2013; Yuill *et al.*, 2016). However, the majority of crevasse splays do not lead to an avulsion of their parent channel. Instead, their activity eventually ceases due to an aggradation-induced decrease in floodwater capacity and backfilling of the crevasse-splay channels (e.g. Roberts, 1997; Slingerland and Smith, 2004).

This study presents a detailed analysis of different stages in the evolution of crevasse splays based on observations made in the distal part of the pristine modern-day Río Colorado dryland fluvial system, fringing the endorheic Altiplano Basin in Bolivia. A generic life cycle is proposed and presented as a key building mechanism in the aggradation of alluvial ridges in low-gradient fluvial fans, and its role in the subsequent autocyclic switching (i.e. avulsion) of the river path is discussed. The semi-arid lowstand basin setting and consequent sub-aerial termination of the studied system allows for an assessment of fluvial processes in the absence of any influence from vegetation, base-level changes, or lateral confinement. Moreover, it can serve as an analogue for gas-bearing Permo-Triassic fluvial successions with high proportions of preserved floodplain deposits along the Central and North Atlantic margins (e.g. Williams and McKie, 2009; Donselaar *et al.*, 2011; McKie, 2011a).

Geological Setting

The Altiplano Basin is a large (~200 000 km^2) north–south elongated endorheic basin that extends across Peru, Bolivia, Argentina, and Chile and is surrounded by the Cordilleran mountain ranges (Figure 1). Tectonically, the basin forms part of the Central Andean ocean-continent convergent margin. The basin is a high-altitude (3650–4200 m above mean sea level) hinterland plateau that formed during the Andean Orogeny (Cretaceous–present) in response to the eastward subduction of the oceanic Nazca Plate under the South American Plate and the related uplift of the Andean orogenic belt (Argollo and Mourguiart, 2000; Horton *et al.*, 2001; Rigsby *et al.*, 2005; Risacher and Fritz, 2009). From the Cretaceous onwards, the basin is filled with volcanoclastics and lacustrine and alluvial sediment (Elger *et al.*, 2005). At present, it lies in the rain shadow of the Eastern Cordillera and has an overall semi-arid climate. Large salt lakes occupy depressions in the southern part of the basin. Towards the north, these pass into ephemeral lakes and a permanent lake (Lago Titicaca) in response to a precipitation gradient across the basin length, from 200 mm yr^{-1} in the south to 800 mm yr^{-1} in the north (Argollo and Mourguiart, 2000). Past wetter climate periods have been recorded; these are characterized by short periods of rapid lake expansion (Servant *et al.*, 1995; Sylvestre *et al.*, 1999; Baker *et al.*, 2001; Fornari *et al.*, 2001; Chepstow-Lusty *et al.*, 2005; Rigsby *et al.*, 2005; Placzek *et al.*, 2006). An example of such wetter climate period is the Tauca phase (26 100–14 900 cal. yr BP), when a large part of the basin was covered with lacustrine water (Donselaar *et al.*, 2013) and the lake level rose to 127 m above the present-day lowstand level (Baker *et al.*, 2001).

The Río Colorado fluvial system on the south-eastern fringe of the Altiplano Basin has its catchment in the Eastern

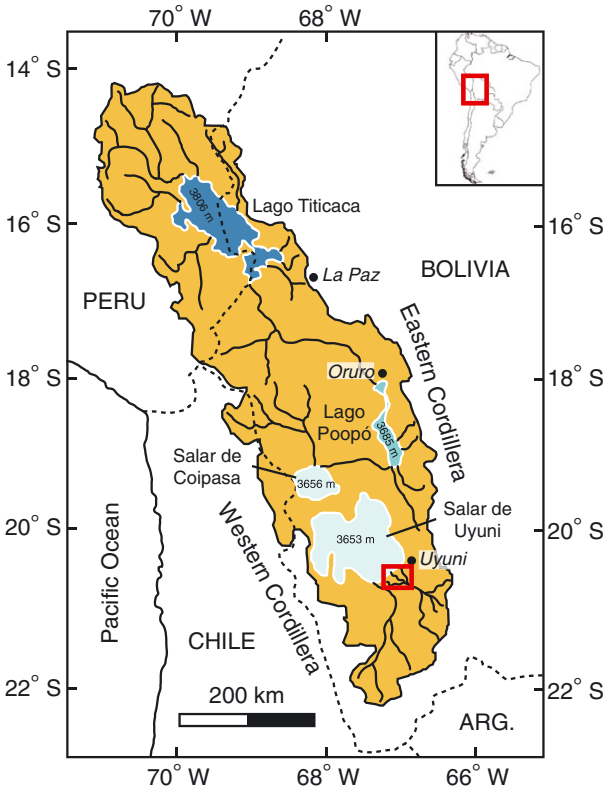

Figure 1. Overview of the Altiplano Basin (yellow) showing the internal drainage pattern, southward decrease in lake water levels (dark to light blue), and study area (red box). Inset: location in South America. Modified from Donselaar *et al.* (2013). [Colour figure can be viewed at wileyonlinelibrary.com]

Cordillera (Figure 2). The river flows to the northwest onto the low-gradient alluvial plain at the edge of the Salar de Uyuni sub-basin, where it is mostly single-thread (Donselaar *et al.*, 2013). Absolute age dating using optically stimulated luminescence (OSL) reveals that the river system has been active for ~12 kyr (Donselaar *et al.*, 2017), gradually prograding towards the salt lake.

Methodology

The study area entails the pristine distal (depositional) part of the Río Colorado fluvial system (Donselaar *et al.*, 2013; Li *et al.*, 2014a; Li and Bristow, 2015), covering an area of ~500 km^2 southwest of the city of Uyuni in the Potosí department of Bolivia (Figures 2 and 3). Field campaigns were carried out in the months of October and November of 2014 and 2016, at the end of the dry (winter) season when the river was at its low-flow stage and the area was best accessible.

Google Earth Pro provided a time-lapse overview of the system morphology over the period 2004–2016 with a maximum resolution of ~0.5 m pixel^{-1} (i.e. *WorldView* and *Quickbird* satellite imagery). Given the high dynamicity of the fluvial environment (Li *et al.*, 2014a), kite aerial photography (KAP; Smith *et al.*, 2009) was employed to obtain contemporary aerial imagery at several locations. This was subsequently used to make georeferenced photogrammetric projections in *Agisoft PhotoScan Pro*. A *Trimble 5700* differential global positioning system (dGPS) set was used to adequately measure subtle floodplain topography with sub-centimetre accuracy (e.g. Parkinson and Enge, 1996; Chan and Baciu, 2012). Sections were recorded using either a hand-held or vehicle-borne setup of the dGPS rover within a <5 km radius from its base station. This yielded detailed elevation profiles of crevasse splays, their channels, and the surrounding floodplain (subject to a structural +44.4 m vertical datum shift relative to Figure 1). All aerial and satellite imagery and dGPS data were combined in a geographic information system (GIS) for comprehensive analysis (Figure 3). Sample pits were dug in order to record sedimentary logs comprising bed thickness, nature of contacts, grain size, colour, and sedimentary structures. Sediment samples were collected for grain-size analyses using a *Helos KR Sympatico* laser particle sizer (Blott *et al.*, 2004), in order to quantify the preserved (i.e. end-member) range in sediment size.

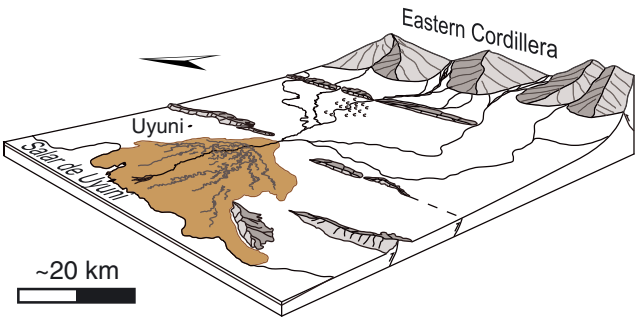

Figure 2. Schematic diagram of the Río Colorado fluvial system. The studied distal (depositional) part is indicated in brown; arrow indicates north. Modified from Donselaar *et al.* (2013). [Colour figure can be viewed at wileyonlinelibrary.com]

Morphological Observations

Three configurations of crevasse splays are distinguished based on their inferred hydrological role: (1) facilitating unidirectional drainage, (2) facilitating bidirectional drainage, and (3) post-active abandonment (Figure 3). These classifications follow from observations of the crevasse-splay channel gradient and relevant geomorphological features.

Unidirectional drainage

Crevasse splays favouring one-directional flow comprise bifurcating and locally-anastomosing low-sinuosity channels with a gradient of up to 4 × 10^{-4} dipping away from the main river and towards the floodplain (Figure 4). These channels are proximally erosive and contain basal scours indicative of outward flow, i.e. away from their parent channel (Figure 5A). Their relative depth and gradient decreases from proximal to distal, leading to an increase in their width-to-depth ratio (Figure 4). Subtle levees (Figure 5B) and elongate terminal lobes

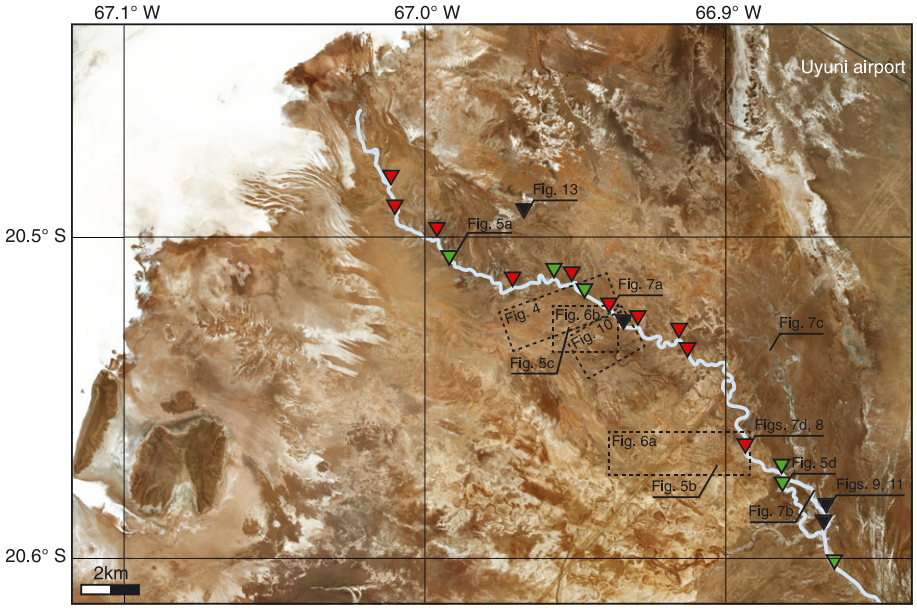

Figure 3. Satellite image of the study area (dated 2017; Bing Maps) showing the single-thread active river (light blue), morphological classification of observed crevasse splays (triangles in green: unidirectional drainage, red: bidirectional drainage, and black: abandoned), and the locations of Figures 4–13. [Colour figure can be viewed at wileyonlinelibrary.com]

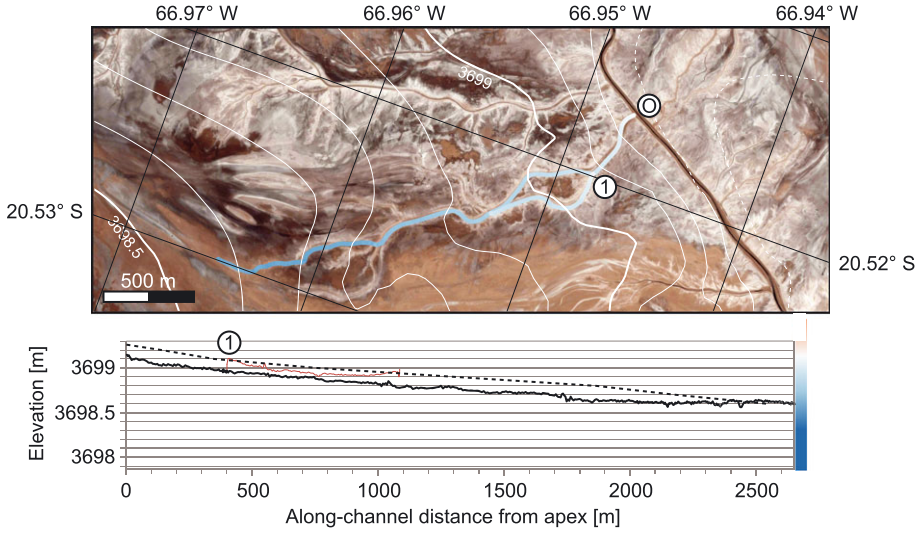

Figure 4. Satellite image (dated March 2016; Google Earth Pro) and along-channel elevation profile of a crevasse splay facilitating unidirectional drainage. The image shows the elevation of the channel floor relative to the apex (coloured lines; see corresponding colour bar next to profile) and dGPS-based surface topography (white contours). The profile shows the along-channel elevation of the first-order (black) and second-order (red; number corresponds to satellite image) channel floor, and the surface topography alongside the first-order channel (dashed line). The *X*-axis origin corresponds to 'O'; *Y*-axis origin is levelled with the parent-channel floor. [Colour figure can be viewed at wileyonlinelibrary.com]

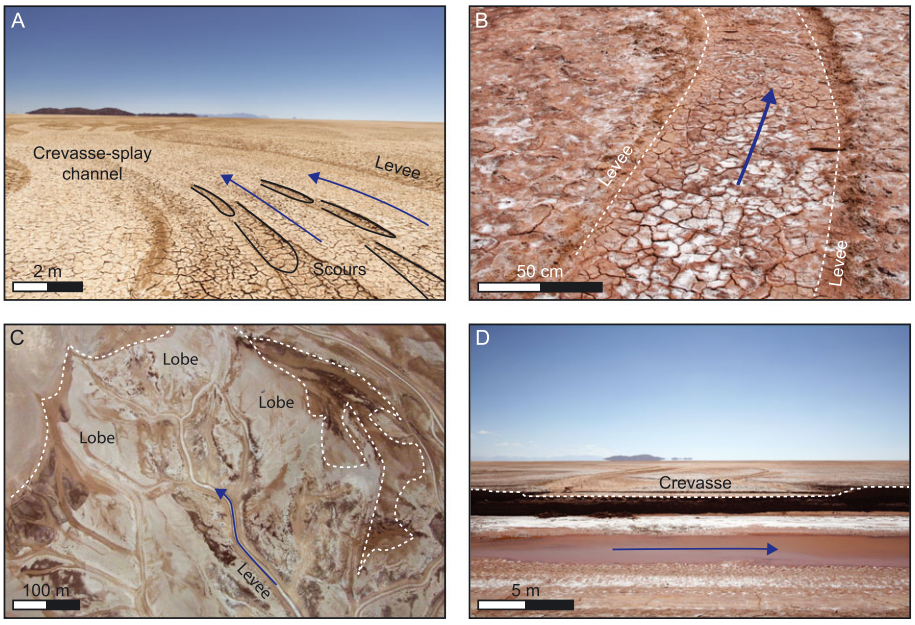

Figure 5. Crevasse splays facilitating unidirectional drainage. Blue arrows indicate flow direction. (A) Scours (~1 dm deep) indicative of flow towards the floodplain. (B) Subtle levees (~1 cm high levee top) alongside a crevasse-splay channel. (C) KAP orthophoto showing levees and amalgamated lobes at the termini of crevasse-splay channels. (D) Crevasse apex seen from its parent channel (unincised cutbank is ~1.4 m high). [Colour figure can be viewed at wileyonlinelibrary.com]

(Figure 5C) occur mainly in the distal part of the crevasse splay, resulting from net deposition alongside and at the end of the channels, respectively. Rill channels are absent and there is no evidence for deposition or return flow at the apex of the crevasse splay (Figure 5D).

Bidirectional drainage

Bidirectional flow in crevasse splays is accommodated by the near-horizontal thalweg of the lower-order crevasse-splay channels, constituting an absence of gradient (0–1.5 × 10^{-4}; Figure 6). These channels are more sinuous than those favouring unidirectional drainage and are generally erosive, especially in the proximal reaches of the crevasse splay where they incise deep into the substrate (Figure 6) which exhibits a subtle gradient (2–4 × 10^{-4}) away from the main river. Basal scours confirm the occurrence of both outflow and reflux (Figure 7A) of floodwater. Higher-order crevasse-splay channels with a hanging floor may have a gradient dipping away from their respective lower-order parent channel, locally showing features associated with outflow of floodwater (Figure 6A). Contrarily, the presence of rill channels with small sediment lobes at their base suggests a reflux of water from the inundated floodplain into the relative depression of crevasse-splay channels (Figures 7B and 7C). The latter occurs on a larger scale at the junction of the apical crevasse and its associated parent channel, where an asymmetric sediment lobe is found in the

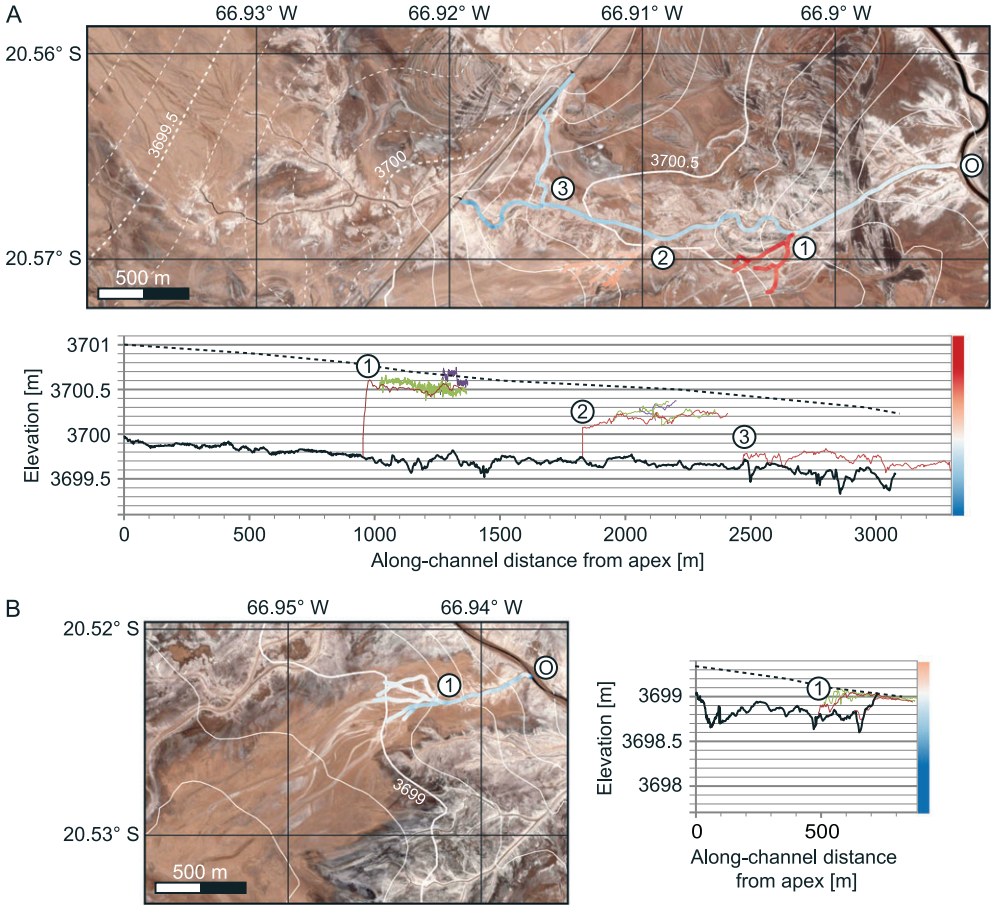

Figure 6. Satellite images (dated March 2016; Google Earth Pro) and along-channel elevation profiles of crevasse splays facilitating bidirectional drainage. The images show the elevation of the channel floor relative to the apex (coloured lines; see corresponding colour bars next to their associated profiles) and dGPS-based surface topography (white contours). The profiles show the along-channel elevation of first-order (black), second-order (red; number corresponds to satellite image), third-order (green), and fourth-order (purple) channel floor, and the surface topography alongside the first-order channel (dashed). The *X*-axis origin corresponds to 'O'; *Y*-axis origin is levelled with the parent-channel floor. (A) Apex has incised significantly deeper (~1 m) into the river bank and the remaining floodplainward gradient is low. Note that the elevation at the termini is still ~0.5 m above the parent-channel floor. (B) Horizontal and partly-reversed channel-floor gradient. [Colour figure can be viewed at wileyonlinelibrary.com]

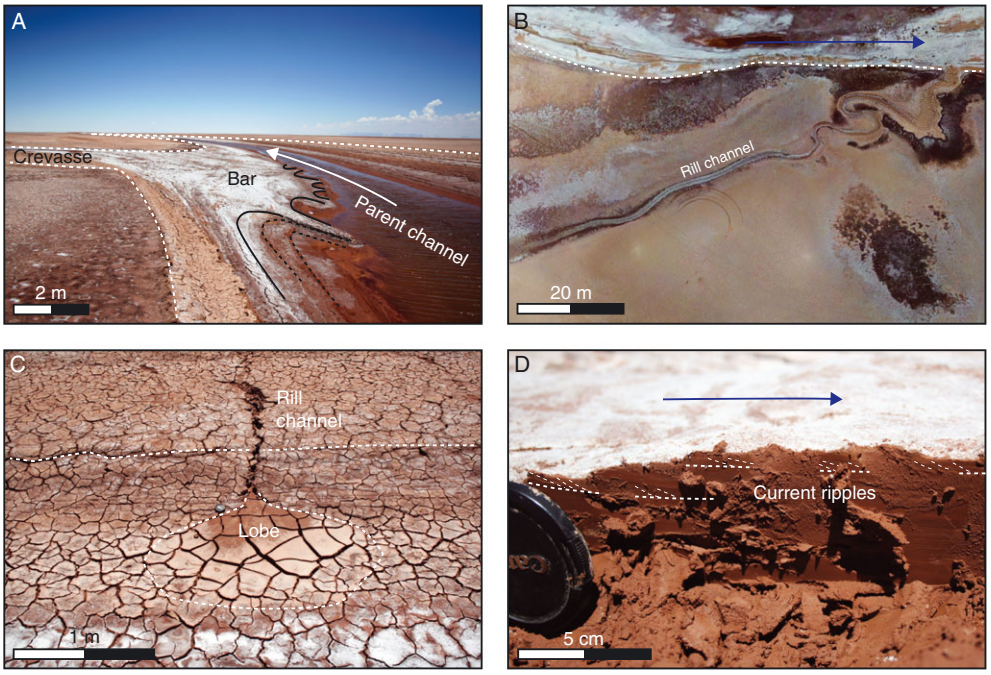

Figure 7. Crevasse splays facilitating bidirectional drainage. White/blue arrows indicate flow direction. (A) Reflux lobe in the parent channel (associated with the crevasse splay in Figure 6B) with scours indicating return flow at the crevasse-splay apex. (B) KAP orthophoto of a sinuous rill channel draining into the main river. (C) Depositional lobe at the base of a rill channel as it enters a channel depression. (D) Current ripples on a reflux lobe (associated with the crevasse splay in Figure 6A). [Colour figure can be viewed at wileyonlinelibrary.com]

main river (Figures 4, 7A and 8). The locus of deposition is partially downstream of the crevasse, causing a local narrowing of the parent channel (Figures 7A and 8). This results in abundant scouring alongside and at the downstream end of the lobe (Figure 8). The upstream part of the lobe is covered by climbing ripples (Figure 7D), ascending its sloped surface oblique to the parent-channel axis as a result of decreasing sediment transport capacity due to flow deceleration.

Abandoned crevasse splays

Ample evidence of abandoned and backfilled crevasse-splay channels is visible in the cut banks of the main river (Figure 9). The surface expression of crevasse splays in this stage is subtle, ranging from planar to convex and with an overall gradient dipping away from the parent channel (Figure 10). Their thickness can range up to 0.25 m for non-channelized sheet deposits proximal to the crevasse-splay channels, thinning towards its distal rims. Remnant depressions of crevasse-splay channels are smoothed out or absent (Figure 10). Accretion surfaces within the fill of these channels (Figure 9) suggest that sediment entered at an angle to their remnant channel axis (i.e. lateral infill). Climbing ripples overlain by clay drapes provide evidence for short periods of channel reactivation (Figure 11), whereas small reflux lobes are also encountered. Preserved grain sizes range from clay to very-fine sand, ~60% of which is silt (cf. Wentworth, 1922) (Figure 12).

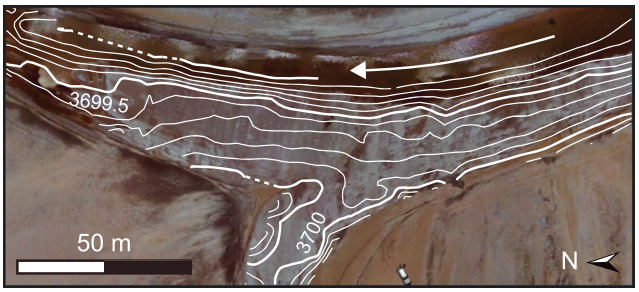

Figure 8. KAP orthophoto of an asymmetrical reflux lobe (associated with the crevasse splay in Figure 6A) showing surface topography (white contours). White arrow indicates flow direction in the parent channel. Arrow indicates north. [Colour figure can be viewed at wileyonlinelibrary.com]

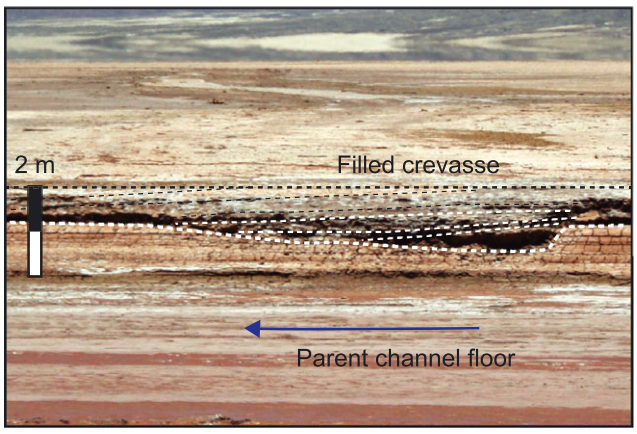

Figure 9. Filled crevasse-splay channel with a hanging channel floor in the banks of its parent channel. Note the inclined surfaces indicating lateral infill. Blue arrow indicates flow direction. [Colour figure can be viewed at wileyonlinelibrary.com]

A distinctive type of derelict crevasse splays is found along the remnant depressions of abandoned river channels. Its channels show evidence of backstepping erosion (Figure 13) and contain basal scours indicative of flow from the floodplain towards the abandoned main channel. The crevasse-splay channel floor steps down, resulting in an overall gradient dipping towards its former apex and the abandoned trunk channel, acting as a floodplain drainage system.

Crevasse-splay Life Cycle

A generic pattern in the development of crevasse splays can be inferred from the observed configurations and their associated mechanisms. The proposed life cycle applies to all crevasse splays in the river system, provided that their parent channel remains active throughout.

Crevassing and splay equilibration

The formation of a crevasse splay is initiated by a levee breach, allowing water to spill onto the adjacent floodplain before the river exceeds bankfull discharge (i.e. preceding unconfined overbank flooding) (Figures 14A and 14B). The floodwater drains from the top part of the main stream, which is undersaturated with sediment (Meselhe *et al.*, 2012), and subsequently encounters a gradient (~2–4 × 10^{-4}) down the outside levee and aggraded fluvial ridge steeper than that of the river profile (8.3 × 10^{-5}; Donselaar *et al.*, 2013). The erosive capacity of the floodwater both deepens and widens the initial crevasse (Yuill *et al.*, 2016), confining outflow at the crevasse-splay apex. Combined with the floodplainward gradient of the substrate, this causes the floodwater to retain its flow energy for longer and transport suspended and newly-eroded sediment further onto the floodplain (cf. Bull, 1979). Crevasse-splay channels incise and stabilize through headward incision, extending from the crevasse-splay apex. Deposition occurs in the distal part of the crevasse splay, causing localized elevation of the floodplain (O'Brien and Wells, 1986; Tooth, 2005) (Figure 14B) which leads to channel bifurcation and switching (Smith *et al.*, 1989; Bristow *et al.*, 1999; Slingerland and Smith, 2004) (Figure 5C).

Proximal erosion and distal deposition allow crevasse-splay channels to adjust their flow path towards a graded equilibrium profile (cf. Mackin, 1948), with the lower-lying floodplain at their distal termini as the local base level. Over the course of consecutive flooding events, the crevasse splay progrades further onto the floodplain (O'Brien and Wells, 1986; Smith *et al.*, 1998; Adams *et al.*, 2004; Bernal *et al.*, 2013; Colombera *et al.*, 2013) to a degree that depends on, e.g. floodplain morphology (i.e. gradient and drainage capacity) and grain size (Millard *et al.*, 2017), and the hydraulic capacity of the crevasse (Yuill *et al.*, 2016). This process lengthens the equilibrium profile of the crevasse-splay channels whilst raising its local base level through distal aggradation, effectively reducing its gradient (Figure 14B).

Reflux and infill

When river discharge recedes to below bankfull capacity following a flooding event (waning flow stage), it drains more efficiently (i.e. its water level falls more rapidly) than the inundated floodplain (e.g. Dalman and Weltje, 2008). The resulting water-surface gradient may not be able to overcome the river levees and its aggraded fluvial ridge, in which case the

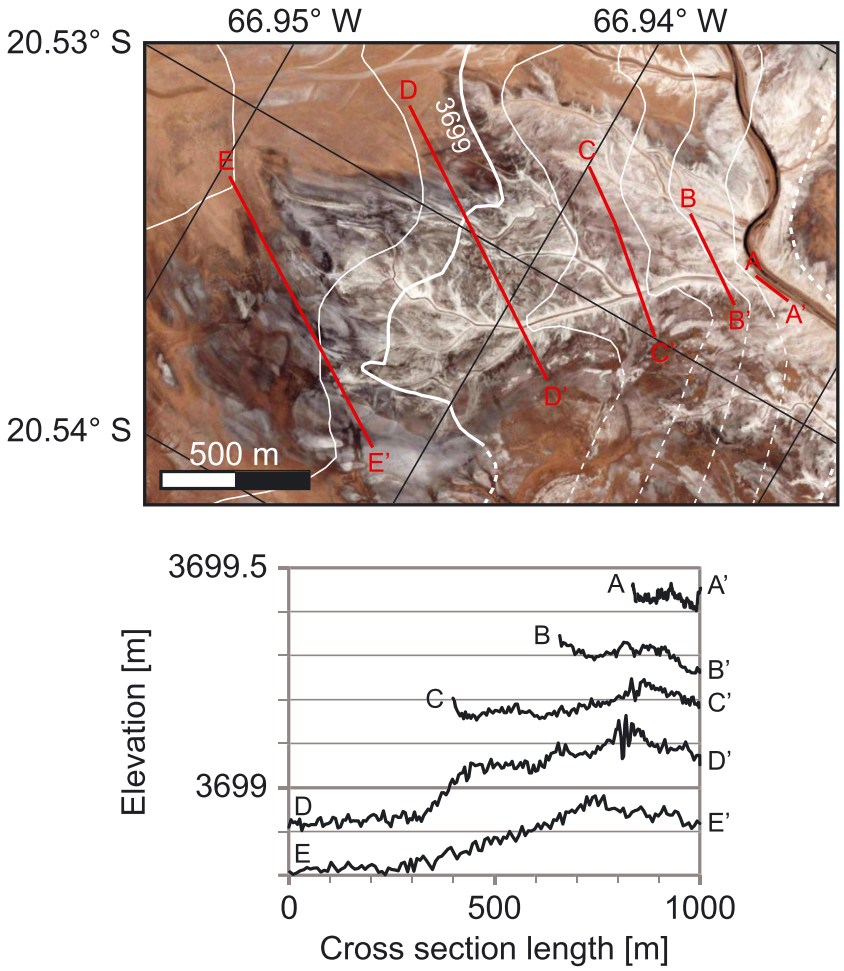

Figure 10. Satellite image (dated March 2016; Google Earth Pro) and elevation profiles of a post-active crevasse splay. The image shows surface topography (white contours) and the location of profiles A–E (in red). The profiles show surface topography from proximal (A–A′) to distal (E–E′). [Colour figure can be viewed at wileyonlinelibrary.com]

floodplain is drained by basinward overland flow and floodwater capture into the remnant depressions of abandoned channels and their derelict crevasse splays (Figure 13), as well as through percolation and evaporation. However, the topographic barrier between the river and the floodplain is locally removed where continued profile equilibration of crevasse-splay channels causes the apical hanging floor of the crevasse to incise deeper than the maximum flooding level (Figure 14 C). The now-unobstructed hydrological gradient induces a return flow of floodwater through the crevasse-splay channels back into the main river.

Undersaturated floodwater re-entering the relative depression of crevasse-splay channels cuts out rill channels in the adjacent splay deposits (O'Brien and Wells, 1986; Zwoliński, 1992; Bridge, 2006), remobilizing sediment and transporting it back towards the main river (Donselaar *et al.*, 2013) (Figure 7C). This return flow causes backstepping erosion at junctions of different-order channels, where the higher-order channel typically has a hanging floor (Figure 6). In-channel redeposition of sediment occurs downstream of each such confluence (i.e. in the lower-order channel). This is most evident at the junction of the crevasse and the main river, where it forms an asymmetrical lobe (Donselaar *et al.*, 2013) (Figures 8 and 14C).

The reflux of floodwater causes the crevasse-splay channel network to adjust towards a reversed equilibrium profile with the trunk-channel floor as its base level, eroding and depositing sediment upstream and downstream of each break in slope (i.e. junction of different-order channels), respectively (Figure 14C). The relative concentration of suspended sediment in successive outflow increases as the hanging floor of the crevasse incises deeper into the main channel bank (Figure 6), causing its erosive potential to decrease (Meselhe *et al.*, 2012). The floodwater decelerates earlier as the crevasse-splay gradient has been reduced or reversed (i.e. no longer exceeds that of the parent channel) by return flow from the preceding flooding event, resulting in in-channel deposition of suspended sediment (cf. Schumm, 1993; Bull, 1997; Field, 2001; Slingerland and Smith, 2004). Over consecutive flooding events, this mechanism fills in the crevasse-channel depressions, effectively shutting down the crevasse splay (Figure 14D).

Preserved overbank sediment

As the process of crevassing implies reworking of levee sediment, the preservation potential of fluvial levees is low where crevassing is abundant. This is in accordance with their under-representation in the rock record, as observed in earlier studies (e.g. Brierley *et al.*, 1997). The majority of preserved crevasse-splay sediment consists of amalgamated splay lobes, fining up in grain size (e.g. Mjøs *et al.*, 1993; Bristow *et al.*, 1999; Fisher *et al.*, 2007; Burns *et al.*, 2017) and blanketed by floodplain fines (Bridge, 2006; McKie, 2011b; Dalman *et al.*, 2015). Crevasse-splay channels constitute a relatively small proportion of preserved sediment, decreasing in proportion from proximal to distal (e.g. Tooth, 2005; Burns *et al.*, 2017). Their fill is heterogeneous (Figure 12), consisting mainly of

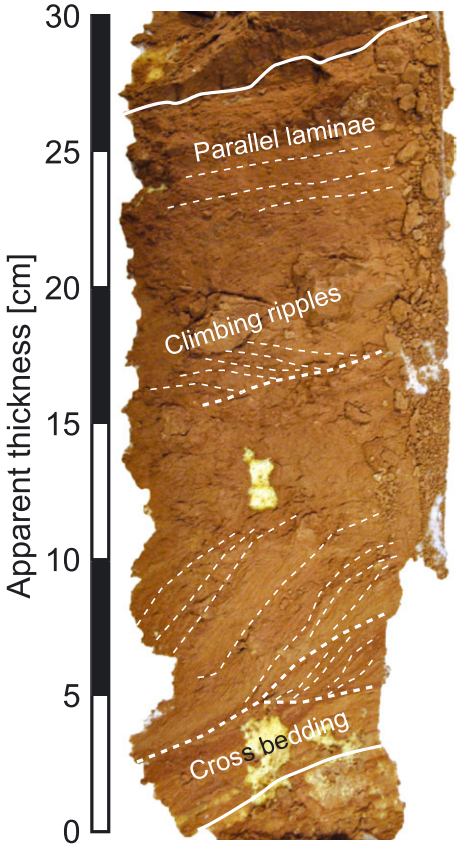

Figure 11. Lacquer peel from a post-active crevasse-splay channel showing sedimentary structures. [Colour figure can be viewed at wileyonlinelibrary.com]

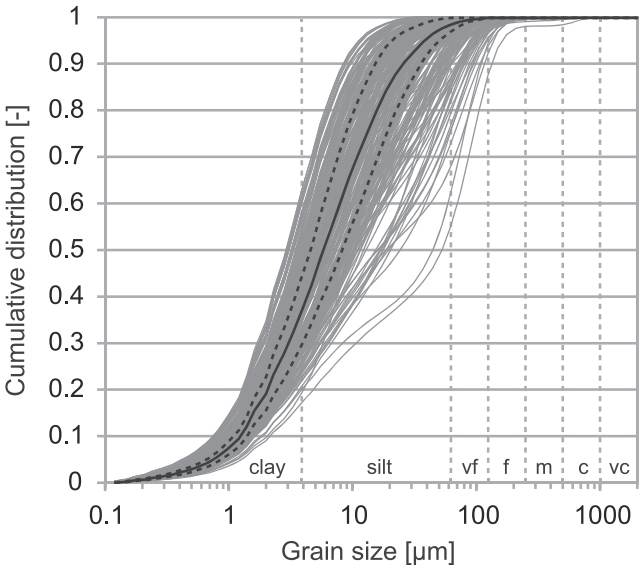

Figure 12. Cumulative distribution of 261 grain-size samples from crevasse splays after laser particle sizer analysis showing the median (black) and the median absolute deviation (MAD; dashed lines). Grain-size classes are indicated with dashed grey lines: very fine (vf), fine (f), medium (m), coarse (c), and very coarse (vc).

sediment (re)deposited under a waning flow regime during outflow (Tooth, 2005), and pelagic floodplain fines (Bristow *et al.*, 1999; Fisher *et al.*, 2007). The preservation potential of deposits associated with return flow of floodwater (i.e. in-channel reflux lobes) is assumedly low due to subsequent erosion by sustained lower-order flow (Figure 14D).

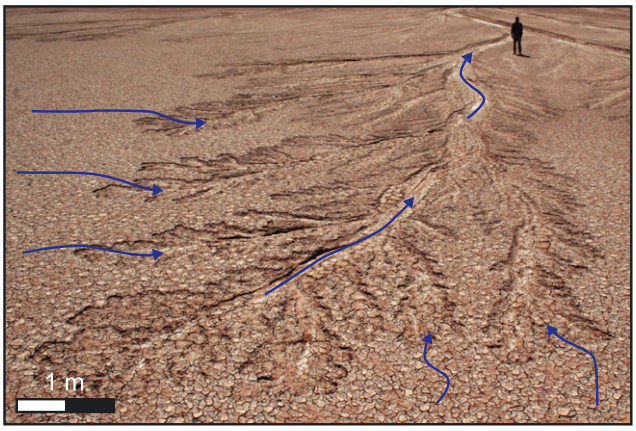

Figure 13. Backstepping erosion in a post-active crevasse splay reused for floodplain drainage into an abandoned channel. Blue arrow indicates flow direction. Person for scale (~1.75 m). [Colour figure can be viewed at wileyonlinelibrary.com]

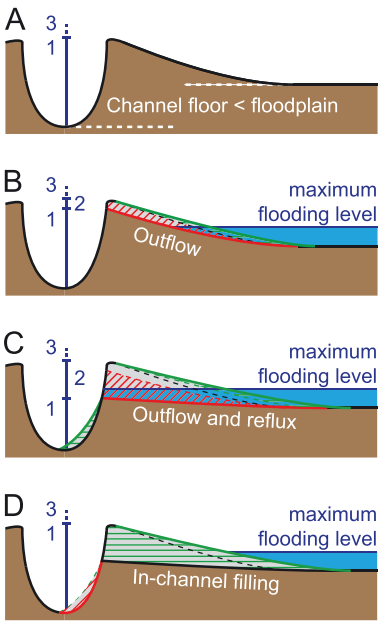

Figure 14. Schematic representation of the generic life cycle of a crevasse splay (not to scale). Incision of the (crevasse-splay) channel floor and adjacent deposition of crevasse-splay levees and lobes is indicated in red and green, respectively. Black dashed line indicates the adjacent floodplain topography. Parent-channel runoff stage is subdivided in confined in-channel flow (1), crevasse-confined flooding (2), and unconfined overbank flooding (3). (A) Parent channel floor elevation is lower than the floodplain adjacent to the fluvial ridge. (B) Levee topping the fluvial ridge is breached, after which the crevasse-splay channel starts incising towards a graded equilibrium profile. Deposition occurs alongside and at the termini of the crevasse-splay channels. As the apex is higher than the maximum flooding level, there is no return flow of floodwater. (C) Continued incision and deposition puts the crevasse apex below the maximum flooding level, facilitating return flow of floodwater and sediment back into the parent channel during the waning stage of flooding, forming a reflux lobe. (D) The reduced gradient causes flow deceleration, leading to in-channel deposition and, ultimately, deactivation of the crevasse splay. The reflux lobe in the parent channel is eroded by sustained lower-order flow. [Colour figure can be viewed at wileyonlinelibrary.com]

Role in Fluvial Aggradation

The deposition of crevasse splays is a principal mechanism for near-channel overbank aggradation in the unconfined distal part of low-gradient fluvial fans, where floodplain sedimentation rates are generally low (e.g. Leeder, 1975; Shen *et al.*, 2015). Their proposed life cycle provides new insights into their role in the aggradation and subsequent abandonment (by avulsion) of alluvial ridges. This ultimately leads to an improved understanding of preserved stratigraphy in fluvial successions with high proportions of floodplain deposits.

Alluvial ridges and avulsion

Over the course of their life cycle, crevasse splays form a decimetre-scale positive relief (i.e. splay) extending up to several square kilometre across the floodplain proximal to the main river. Consecutive crevasse splays interact with adjacent splays in a process of compensational stacking (Donselaar *et al.*, 2013; Li *et al.*, 2014a), amalgamating in their erosive proximal reaches and conformably onlapping towards their distal fringes. This mechanism creates a continuous elevated rim alongside the main river, laterally expanding levee topography through redeposition and establishing a fluvial ridge up to several kilometres wide. The consequent rise in bankfull height of the main river corresponds to the aggradation of its channel floor, assuming that its local hydraulic capacity remains more or less constant (Van Toorenenburg *et al.*, 2016). Episodes of unconfined overbank flow continue to deposit levees on top of the aggrading alluvial ridge. These are in turn redeposited by crevasse splays prograding over their precursors off a gradually-increasing slope (Van Toorenenburg *et al.*, 2016). This vertical stacking of crevasse splays prolongs the aggradation of the alluvial ridge, which becomes increasingly perched above the distant floodplain (Figure 15A).

Given that its parent channel remains active, each crevasse splay will complete its entire life cycle on the condition that its crevasse-splay channels do not incise down to the channel floor of its parent river (i.e. remain hanging). This is dependent upon the elevation of the distal termini (i.e. local base level) of the crevasse-splay channels relative to that of their trunk channel. When the thalweg of the parent river has super-elevated to above the distal reach of a crevasse splay, equilibration of the crevasse-splay channels ultimately leads to headward incision down to or below its channel floor. At the same time, the crevasse splay will capture an increasing proportion of the total discharge and sediment, accelerating its development. If the gradient of one or more crevasse-splay channels has remained steeper than that of the main channel once incision reaches its channel floor, the river avulses (i.e. low-flow stage discharge is rerouted through the crevasse splay) (Figure 15B). This process is amplified by backwater effects induced by the downstream reduction in hydraulic capacity of the main river (e.g. flow constriction by in-channel reflux deposits). The proposed mechanisms are in accordance with the avulsion criteria suggested by Mohrig *et al.* (2000), Slingerland and Smith (2004), and Dalman and Weltje (2008), as summarized in a review by Hajek and Wolinsky (2012).

Generic relevance and limitations

The mechanisms proposed in this study exclusively concern self-regulating fluvial processes. The specific configuration of the observed Río Colorado fluvial fan eliminates any significant influence from external factors such as vegetation (barren floodplain), lateral constraint (unconfined alluvial plain), or base-level change (lowstand endorheic basin). The dryland character of the system favours a single-thread river decreasing in hydraulic capacity downstream (e.g. North and Warwick, 2007; Donselaar *et al.*, 2013), preventing multi-channel interference and promoting overbank deposition. The system autogenically generates accommodation space by progradating across the low-gradient basin fringe, and its subaerial termination ensures that all sediment is captured, allowing for a comprehensive account of its distribution.

The mechanisms proposed in this study are relevant to fluvial settings that facilitate progradational avulsions (cf. Hajek and Edmonds, 2014). Floodplain aggradation (and preservation) in such environments requires positive accommodation space in a relatively low-energy environment (i.e. low-gradient and unconfined) (Nichols and Fisher, 2007). The subsequent occurrence of crevasse splays is promoted by relatively coarse-grained suspended sediment (during peak runoff) and effective floodplain drainage (Millard *et al.*, 2017).

In humid environments, river discharge variations are significantly smaller than those in arid or semi-arid settings (McMahon *et al.*, 1987), stream capacity does not decrease downstream (Tooth, 2000), and vegetation may increase bank stability (Simon and Collinson, 2002). Although this may moderate the frequency of flooding and the occurrence of crevasse splays, it does not change the inherently-episodic mechanism of crevasse-splay channels adjusting to a graded equilibrium

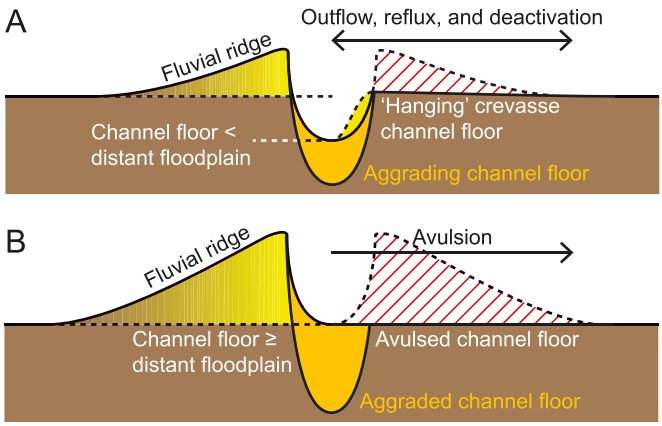

Figure 15. Schematic cross-section of an aggrading fluvial ridge (not to scale). Maximum incision of the crevasse-splay channel floor is indicated in red. (A) As long as the crevasse-splay channel floor remains 'hanging', the crevasse splay will complete its life cycle (Figure 14). (B) Upon reaching critical super elevation, the river avulses through the active crevasse-splay channel, reaching onto a low-lying part of the floodplain. [Colour figure can be viewed at wileyonlinelibrary.com]

profile and, hence, the life cycle proposed in this study. However, floodplain morphodynamics (i.e. availability of accommodation space and drainage conditions) may be significantly influenced by non-depositional factors such as prolific vegetation and ponding of floodwater (Millard *et al.*, 2017).

Implications for connected sand volumes

Given their relatively rapid accumulation rate and high preservation potential, crevasse splays form an important constituent of stratigraphy associated with the distal part of low-gradient fluvial fans, for which the studied system qualifies as a modern-day analogue. Comprising sand and silt, their contribution to connected sand volumes (which may constitute hydrocarbon reservoirs) has been acknowledged in previous studies (e.g. Jordan and Pryor, 1992; Pranter *et al.*, 2008; McKie, 2011b), albeit to a limited extent. The heterolithic fill of crevasse-splay channels connects individual splays to their coeval trunk channel, which constitutes the main hydrocarbon reservoir. The proposed role of crevasse splays in building alluvial ridges entails lateral amalgamation and vertical stacking of individual units, creating sand-on-sand contact. This implies that fluvial ridges comprise interconnected crevasse splays, combining into large connected sediment volumes. Truncation of fluvial deposits by younger channels may further enhance connectivity. These inferences are in accordance with the nature and types of crevasse-splay connectivity described by Van Toorenenburg *et al.* (2016), based on observations in outcrop stratigraphy. Crevasse splays effectively connect otherwise-isolated channel deposits, even when their deposition was not coeval. They should therefore be included in net volume estimations and production models of fluvial successions that contain hydrocarbon reservoirs in order to avoid underestimations.

Conclusions

A generic life cycle applies to crevasse splays in aggrading alluvial ridges, generally spanning multiple flooding events. Initial development is dominantly controlled by the outflow of floodwater, promoting erosion near the crevasse apex and deposition towards the splay fringes as the crevasse-splay channels adjust towards a graded equilibrium profile with their distal termini acting as a local base level. When proximal incision advances to below the maximum level of floodplain inundation, return flow occurs during the waning stage of flooding. This floodwater reflux leads to a temporary repositioning of the local base level to the deeper trunk channel thalweg and consequent reversal of the graded equilibrium profile. The resultant decrease in crevasse-splay channel gradient ultimately leads to backfilling and abandonment of the crevasse splay.

Consecutive crevasse splays form an alluvial ridge through lateral amalgamation and subsequent vertical stacking. As the alluvial ridge becomes increasingly perched above the distant floodplain, splay equilibration may cause incision of the levee crevasse down to or below its trunk channel thalweg, leading to an avulsion.

The mechanisms proposed in this study are relevant to fluvial settings promoting progradational avulsions. The relatively rapid accumulation rate and high preservation potential of crevasse splays in this setting makes them an important constituent of the resultant fluvial stratigraphy. Hence, their contribution to net sand volumes in hydrocarbon bearing successions should be considered.

Acknowledgements—This study was supported by ENGIE E&P NL B.V. and Energiebeheer Nederland B.V. (EBN). Carlos Jimenez, Niels Noordijk, Christian Perdomo, Yadir Torres, and Rosmar Villegas assisted in the acquisition and analysis of fieldwork data. Hans van der Marel supplied dGPS sets and consultation. Maarten Prins (VU Amsterdam) provided facilities for the grain-size analysis. The authors are grateful for the constructive reviews by Kathryn Amos and Colin North, whose comments were instrumental in conveying the wider relevance and limitations of the work.

References

Adams PN, Slingerland RL, Smith ND. 2004. Variations in natural levee morphology in anastomosed channel flood plain complexes. *Geomorphology* **61**: 127–142. https://doi.org/10.1016/j.geomorph.2003.10.005.

Anderson DS. 2005. Architecture of crevasse splay and point-bar bodies of the nonmarine Iles Formation north of Rangely, Colorado: implications for reservoir description. *The Mountain Geologist* **42**: 109–122.

Argollo J, Mourguiart P. 2000. Late Quaternary climate history of the Bolivian Altiplano. *Quaternary International* **72**: 37–51.

Arndorfer DJ. 1973. Discharge patterns in two crevasses on the Mississippi River delta. *Marine Geology* **15**: 269–287.

Baker PA, Rigsby CA, Seltzer GO, Fritz SC, Lowenstein TK, Bacher NP, Veliz C. 2001. Tropical climate changes at millennial and orbital timescales on the Bolivian Altiplano. *Nature* **409**: 698–701.

Bernal C, Christophoul F, Darrozes J, Laraque A, Bourrel L, Soula JC, Guyot JL, Baby P. 2013. Crevassing and capture by floodplain drains as a cause of partial avulsion and anastomosis (lower Rio Pastaza, Peru). *Journal of South American Earth Sciences* **44**: 63–74. https://doi.org/10.1016/j.jsames.2012.11.009.

Blott SJ, Croft DJ, Pye K, Saye SE, Wilson HE. 2004. Particle size analysis by laser diffraction. In *Forensic Geoscience: Principles, Techniques and Applications*, Pye K, Croft DJ (eds) . Geological Society: London; 63–73. Special Publication 232

Bridge JS. 2006. Fluvial facies models: recent developments. In *Facies Models Revisited*, Posamentier HW, Walker RG (eds) . SEPM: Tulsa, OK; 85–170. SEPM Special Publication 84

Brierley GJ, Ferguson RJ, Woolfe KJ. 1997. What is a fluvial levee? *Sedimentary Geology* **114**: 1–9. https://doi.org/10.1016/S0037-0738(97)00114-0.

Bristow CS, Skelly RL, Ethridge FG. 1999. Crevasse splays from the rapidly aggrading, sand-bed, braided Niobrara River, Nebraska: effect of base-level rise. *Sedimentology* **46**: 1029–1047. https://doi.org/10.1046/j.1365-3091.1999.00263.x.

Buehler HA, Weissmann GS, Scuderi LA, Hartley AJ. 2011. Spatial and temporal evolution of an avulsion on the Taquari River distributive fluvial system from satellite image analysis. *Journal of Sedimentary Research* **81**: 630–640. https://doi.org/10.2110/jsr.2011.040.

Bull WB. 1979. Threshold of critical power in streams. *Geological Society of America Bulletin* **90**: 453–464. https://doi.org/10.1130/0016-7606(1979)90%3C453.

Bull WB. 1997. Discontinuous ephemeral streams. *Geomorphology* **19**: 227–276. https://doi.org/10.1016/S0169-555X(97)00016-0.

Burns C, Mountney NP, Hodgson DM, Colombera L. 2017. Anatomy and dimensions of fluvial crevasse-splay deposits: examples from the Cretaceous Castlegate Sandstone and Neslen Formation, Utah, U.S.A. *Sedimentary Geology* **351**: 21–35. https://doi.org/10.1016/j.sedgeo.2017.02.003.

Cahoon DR, White DA, Lynch JC. 2011. Sediment infilling and wetland formation dynamics in an active crevasse splay of the Mississippi River delta. *Geomorphology* **131**: 57–68. https://doi.org/10.1016/j.geomorph.2010.12.002.

Chan ECL, Baciu G. 2012. Differential GPS and assisted GPS. In *Introduction to Wireless Localization*, Chan ECL, Baciu G (eds). John Wiley & Sons: Singapore; 157–184.

Chepstow-Lusty A, Bush MB, Frogley MR, Baker PA, Fritz SC, Aronson J. 2005. Vegetation and climate change on the Bolivian Altiplano between 108,000 and 18,000 yr ago. *Quaternary Research* **63**: 90–98. https://doi.org/10.1016/j.yqres.2004.09.008.

Colombera L, Mountney NP, Mccaffrey WD. 2013. A quantitative approach to fluvial facies models: methods and example results. *Sedimentology* **60**: 1526–1558. https://doi.org/10.1111/sed.12050.

Dalman RAF, Weltje GJ. 2008. Sub-grid parameterisation of fluvio-deltaic processes and architecture in a basin-scale stratigraphic model. *Computers and Geosciences* **34**: 1370–1380. https://doi.org/10.1016/j.cageo.2008.02.005.

Dalman RAF, Weltje GJ, Karamitopoulos P. 2015. High-resolution sequence stratigraphy of fluvio–deltaic systems: prospects of system-wide chronostratigraphic correlation. *Earth and Planetary Science Letters* **412**: 10–17. https://doi.org/10.1016/j.epsl.2014.12.030.

Donselaar ME, Cuevas Gozalo MC, Moyano S. 2013. Avulsion processes at the terminus of low-gradient semi-arid fluvial systems: lessons from the Río Colorado, Altiplano endorheic basin, Bolivia. *Sedimentary Geology* **283**: 1–14. https://doi.org/10.1016/j.sedgeo.2012.10.007.

Donselaar ME, Cuevas Gozalo MC, Wallinga J. 2017. Avulsion history of a Holocene semi-arid river system – outcrop analogue for thin-bedded fluvial reservoirs in the Rotliegend Feather Edge. *Proceedings, 79th EAGE Conference and Exhibition*. European Association of Geoscientists & Engineers (EAGE): Houten.

Donselaar ME, Overeem I, Reichwein JHC, Visser CA. 2011. Mapping of fluvial fairways in the Ten Boer Member,Southern Permian Basin. In *The Permian Rotliegend of the Netherlands*, Grötsch J, Gaupp R (eds) . SEPM: Tulsa, OK; 105–117. SEPM Special Publication 98

Elger K, Oncken O, Glodny J. 2005. Plateau-style accumulation of deformation: Southern Altiplano. *Tectonics* **24** TC4020. https://doi.org/10.1029/2004TC001675.

Farrell KM. 2001. Geomorphology, facies architecture, and high-resolution, non-marine sequence stratigraphy in avulsion deposits, Cumberland Marshes, Saskatchewan. *Sedimentary Geology* **139**: 93–150. https://doi.org/10.1016/S0037-0738(00)00150-0.

Field J. 2001. Channel avulsion on alluvial fans in southern Arizona. *Geomorphology* **37**: 93–104. https://doi.org/10.1016/S0169-555X(00)00064-7.

Fisher JA, Nichols GJ, Waltham DA. 2007. Unconfined flow deposits in distal sectors of fluvial distributary systems: examples from the Miocene Luna and Huesca Systems, northern Spain. *Sedimentary Geology* **195**: 55–73. https://doi.org/10.1016/j.sedgeo.2006.07.005.

Ford GL, Pyles DR. 2014. A hierarchical approach for evaluating fluvial systems: Architectural analysis and sequential evolution of the high net-sand content, middle Wasatch Formation, Uinta Basin, Utah. *AAPG Bulletin* **98**: 1273–1304. https://doi.org/10.1306/12171313052.

Fornari M, Risacher F, Féraud G. 2001. Dating of paleolakes in the central Altiplano of Bolivia. *Palaeogeography, Palaeoclimatology, Palaeoecology* **172**: 269–282.

Ghazi S, Mountney NP. 2009. Facies and architectural element analysis of a meandering fluvial succession: the Permian Warchha Sandstone, Salt Range, Pakistan. *Sedimentary Geology* **221**: 99–126. https://doi.org/10.1016/j.sedgeo.2009.08.002.

Gulliford AR, Flint SS, Hodgson DM. 2014. Testing applicability of models of distributive fluvial systems or trunk rivers in ephemeral systems: reconstructing 3-D fluvial architecture in the Beaufort Group, South Africa. *Journal of Sedimentary Research* **84**: 1147–1169.

Hajek EA, Edmonds DA. 2014. Is river avulsion style controlled by floodplain morphodynamics? *Geology* **42**: 199–202. https://doi.org/10.1130/G35045.1.

Hajek EA, Wolinsky MA. 2012. Simplified process modeling of river avulsion and alluvial architecture: connecting models and field data. *Sedimentary Geology* **257–260**: 1–30. https://doi.org/10.1016/j.sedgeo.2011.09.005.

Hampton BA, Horton BK. 2007. Sheetflow fluvial processes in a rapidly subsiding basin, Altiplano plateau, Bolivia. *Sedimentology* **54**: 1121–1147. https://doi.org/10.1111/j.1365-3091.2007.00875.x.

Hornung J, Aigner T. 1999. Reservoir and aquifer characterization of fluvial architectural elements: Stubensandstein, Upper Triassic, southwest Germany. *Sedimentary Geology* **129**: 215–280. https://doi.org/10.1016/S0037-0738(99)00103-7.

Horton BK, Hampton BA, Waanders GL. 2001. Paleogene synorogenic sedimentation in the Altiplano plateau and implications for initial mountain building in the central Andes. *GSA Bulletin* **113**: 1387–1400.

Joeckel RM, Tucker ST, McMullin JD. 2016. Morphosedimentary features from a major flood on a small, lower-sinuosity, single-thread river: the unknown quantity of overbank deposition, historical-change context, and comparisons with a multichannel river. *Sedimentary Geology* **343**: 18–37. https://doi.org/10.1016/j.sedgeo.2016.07.010.

Jones HL, Hajek EA. 2007. Characterizing avulsion stratigraphy in ancient alluvial deposits. *Sedimentary Geology* **202**: 124–137. https://doi.org/10.1016/j.sedgeo.2007.02.003.

Jordan DW, Pryor WA. 1992. Hierarchical levels of heterogeneity in a Mississippi River meander belt and application to reservoir systems. *AAPG Bulletin* **76**: 1601–1624. https://doi.org/10.1306/BDFF8A6A-1718-11D7-8645000102C1865D.

Keeton GI, Pranter MJ, Cole RD, Gustason ER. 2015. Stratigraphic architecture of fluvial deposits from borehole images, spectral-gamma-ray response, and outcrop analogs, Piceance Basin, Colorado. *AAPG Bulletin* **99**: 1929–1956. https://doi.org/10.1306/05071514025.

Keller EA, Swanson FJ. 1979. Effects of large organic material on channel form and fluvial processes. *Earth Surface Processes and Landforms* **4**: 361–380. https://doi.org/10.1002/esp.3290040406.

Kleinhans MG, Ferguson RI, Lane SN, Hardy RJ. 2013. Splitting rivers at their seams: bifurcations and avulsion. *Earth Surface Processes and Landforms* **38**: 47–61. https://doi.org/10.1002/esp.3268.

Leeder MR. 1975. Pedogenic carbonates and flood sediment accretion rates: a quantative model for alluvial arid-zone lithofacies. *Geological Magazine* **112**: 257–270.

Li J, Bristow CS. 2015. Crevasse splay morphodynamics in a dryland river terminus: Río Colorado in Salar de Uyuni Bolivia. *Quaternary International* **377**: 71–82. https://doi.org/10.1016/j.quaint.2014.11.066.

Li J, Donselaar ME, Hosseini Aria SE, Koenders R, Oyen AM. 2014a. Landsat imagery-based visualization of the geomorphological development at the terminus of a dryland river system. *Quaternary International* **352**: 100–110. https://doi.org/10.1016/j.quaint.2014.06.041.

Li J, Menenti M, Mousivand A, Luthi SM. 2014b. Non-vegetated playa morphodynamics using multi-temporal Landsat imagery in a semi-arid endorheic basin: Salar de Uyuni, Bolivia. *Remote Sensing* **6**: 10131–10151. https://doi.org/10.3390/rs61010131.

Mackin JH. 1948. Concept of the graded river. *Geological Society of America Bulletin* **59**: 463–512.

McKie T. 2011a. A comparison of modern dryland depositional systems with the Rotliegend group in the Netherlands. In *The Permian Rotliegend of the Netherlands*, Grötsch J, Gaupp R (eds) . SEPM: Tulsa, OK; 89–103. SEPM Special Publication 98

McKie T. 2011b. Architecture and behavior of dryland fluvial reservoirs, Triassic Skagerrak Formation, Central North Sea. In *From River to Rock Record: The Preservation of Fluvial Sediments and Their Subsequent Interpretation*, Davidson SK, Leleu S, North CP (eds). SEPM: Tulsa, OK; 189–214. SEPM Special Publication 97

McMahon T, Finlayson BL, Haines A, Srikanthan R. 1987. Runoff variability: a global perspective. In *The Influence of Climate Change and Climate Variability on the Hydrologic Regime and Water Resources*, Solomon SI, Beran M, Hogg W (eds) . IAHS Press: Wallingford; 3–12. International Association of Hydrological Sciences (IAHS) Publication 168

Meselhe EA, Georgiou I, Allison MA, McCorquodale JA. 2012. Numerical modeling of hydrodynamics and sediment transport in lower Mississippi at a proposed delta building diversion. *Journal of Hydrology* **472–473**: 340–354. https://doi.org/10.1016/j.jhydrol.2012.09.043.

Millard C, Hajek EA, Edmonds DA. 2017. Evaluating controls on crevasse-splay size: implications for floodplain-basin filling. *Journal of Sedimentary Research* **87**: 722–739. https://doi.org/10.2110/jsr.2017.40.

Mjøs R, Walderhaug O, Prestholm E. 1993. Crevasse splay sandstone geometries in the Middle Jurassic Ravenscar Group of Yorkshire, UK. In *Alluvial Sedimentation*, Marzo M, Puigdefabregas C (eds) . International Association of Sedimentologists: Gent; 167–184.Special Publication of the International Association of Sedimentologists 17

Mohrig D, Heller PL, Paola C, Lyons WJ. 2000. Interpreting avulsion process from ancient alluvial sequences: Guadalope-Mantarranya system (northern Spain) and Wasatch Formation (western Colorado). *Geological Society of America Bulletin* **112**: 1787–1803.

Nicholas AP, Walling DE. 1997. Modelling flood hydraulics and overbank deposition on river floodplains. *Earth Surface Processes and Landforms* **22**: 59–77. https://doi.org/10.1002/(SICI)1096-9837(199701)22:1%3C59::AID-ESP652%3E3.0.CO;2-R.

Nichols GJ, Fisher JA. 2007. Processes, facies and architecture of fluvial distributary system deposits. *Sedimentary Geology* **195**: 75–90. https://doi.org/10.1016/j.sedgeo.2006.07.004.

North CP, Warwick GL. 2007. Fluvial fans: myths, misconceptions, and the end of the terminal-fan model. *Journal of Sedimentary Research* **77**: 693–701. https://doi.org/10.2110/jsr.2007.072.

O'Brien PE, Wells AT. 1986. A small, alluvial crevasse splay. *Journal of Sedimentary Research* **56**: 876–879. https://doi.org/10.1306/212F8A71-2B24-11D7-8648000102C1865D.

Parkinson BW, Enge PK. 1996. Differential GPS. In *Global Positioning System: Theory and Applications 2*, Parkinson BW, Spilker JJ, Jr (eds). American Institute of Aeronautics and Astronautics: Reston, VA; 3–50.

Pérez-Arlucea M, Smith ND. 1999. Depositional patterns following the 1870s avulsion of the Saskatchewan River (Cumberland Marshes, Saskatchewan, Canada). *Journal of Sedimentary Research* **69**: 62–73. https://doi.org/10.2110/jsr.69.62.

Placzek C, Quade J, Patchett PJ. 2006. Geochronology and stratigraphy of late Pleistocene lake cycles on the southern Bolivian Altiplano: implications for causes of tropical climate change. *GSA Bulletin* **118**: 515–532. https://doi.org/10.1130/B2577.

Platt NH, Keller B. 1992. Distal alluvial deposits in a foreland basin setting – the Lower Freshwater Molasse (Lower Miocene), Switzerland: sedimentology, architecture and palaeosols. *Sedimentology* **39**: 545–565. https://doi.org/10.1111/j.1365-3091.1992.tb02136.x.

Pranter MJ, Cole RD, Panjaitan H, Sommer NK. 2009. Sandstone-body dimensions in a lower coastal-plain depositional setting: Lower Williams Fork Formation, Coal Canyon, Piceance Basin, Colorado. *AAPG Bulletin* **93**: 1379–1401. https://doi.org/10.1306/06240908173.

Pranter MJ, Vargas MF, Davis TL. 2008. Characterization and 3D reservoir modelling of fluvial sandstones of the Williams Fork Formation, Rulison Field, Piceance Basin, Colorado, USA. *Journal of Geophysics and Engineering* **5**: 158–172. https://doi.org/10.1088/1742-2132/5/2/003.

Rigsby CA, Bradbury JP, Baker PA, Rollins SM, Warren MR. 2005. Late Quaternary palaeolakes, rivers, and wetlands on the Bolivian Altiplano and their palaeoclimatic implications. *Journal of Quaternary Science* **20**: 671–691. https://doi.org/10.1002/jqs.986.

Risacher F, Fritz B. 2009. Origin of Salts and Brine Evolution of Bolivian and Chilean Salars. *Aquatic Geochemistry* **15**: 123–157. https://doi.org/10.1007/s10498-008-9056-x.

Roberts HH. 1997. Dynamic changes of the Holocene Mississippi River delta plain: the delta cycle. *Journal of Coastal Research* **13**: 605–627.

Sahoo H, Gani MR, Hampson GJ, Gani ND, Ranson A. 2016. Facies- to sandbody-scale heterogeneity in a tight-gas fluvial reservoir analog: Blackhawk Formation, Wasatch Plateau, Utah, USA. *Marine and Petroleum Geology* **78**: 48–69. https://doi.org/10.1016/j.marpetgeo.2016.02.005.

Schumm SA. 1993. River Response to Baselevel Change: Implications for Sequence Stratigraphy. *Journal of Geology* **101**: 279–294. https://doi.org/10.1086/648221.

Servant M, Fournier M, Argollo J, Servant-Vildary S, Sylvestre F, Wirrmann D, Ybert JP. 1995. La dernière transition glaciaire/interglaciaire des Andes tropicales sud (Bolivie) d'après l'Étude des variations des niveaux …. *Comptes Rendus de l'Académie des Sciences, Paris, Séries II* **320**: 729–736.

Sheets BA, Hickson TA, Paola C. 2002. Assembling the stratigraphic record: depositional patterns and time-scales in an experimental alluvial basin. *Basin Research* **14**: 287–301. https://doi.org/10.1046/j.1365-2117.2002.00185.x.

Shen Z, Törnqvist TE, Mauz B, Chamberlain EL, Nijhuis AG, Sandoval L. 2015. Episodic overbank deposition as a dominant mechanism of floodplain and delta-plain aggradation. *Geology* **43**: 875–878. https://doi.org/10.1130/G36847.1.

Simon A, Collinson AJC. 2002. Quantifying the mechanical and hydrological effects of riparian vegetation on streambank stability. *Earth Surface Processes and Landforms* **27**: 527–546. https://doi.org/10.1002/esp.325.

Slingerland RL, Smith ND. 2004. River avulsions and their deposits. *Annual Review of Earth and Planetary Sciences* **32**: 257–285. https://doi.org/10.1146/annurev.earth.32.101802.120201.

Smith JS, Chandler J, Rose J. 2009. High spatial resolution data acquisition for the geosciences: kite aerial photography. *Earth Surface Processes and Landforms* **34**: 155–161. https://doi.org/10.1002/esp.

Smith ND, Cross TA, Dufficy JP, Clough SR. 1989. Anatomy of an avulsion. *Sedimentology* **36**: 1–23.

Smith ND, Pérez-Arlucea M. 1994. Fine-grained splay deposition in the avulsion belt of the lower Saskatchewan River, Canada. *Journal of Sedimentary Research* **64**: 159–168. https://doi.org/10.1306/D4267F7D-2B26-11D7-8648000102C1865D.

Smith ND, Slingerland RL, Pérez-Arlucea M, Morozova GS. 1998. The 1870s avulsion of the Saskatchewan River. *Canadian Journal of Earth Sciences* **35**: 453–466. https://doi.org/10.1139/e97-113.

Sylvestre F, Servant M, Servant-Vildary S, Causse C, Fournier M. 1999. Lake-level chronology on the Southern Bolivian Altiplano (18°–23° S) during Late-Glacial Time and the Early Holocene. *Quaternary Research* **51**: 54–66. https://doi.org/10.1006/qres.1998.2017.

Van Gelder A, Van den Berg JH, Cheng G, Xue C. 1994. Overbank and channelfill deposits of the modern Yellow River delta. *Sedimentary Geology* **90**: 293–305.

Van Toorenenburg KA, Donselaar ME, Noordijk NA, Weltje GJ. 2016. On the origin of crevasse-splay amalgamation in the Huesca fluvial fan (Ebro Basin, Spain): implications for connectivity in low net-to-gross fluvial deposits. *Sedimentary Geology* **343**: 156–164. https://doi.org/10.1016/j.sedgeo.2016.08.008.

Tooth S. 2000. Process, form and change in dryland rivers: a review of recent research. *Earth-Science Reviews* **51**: 67–107.

Tooth S. 2005. Splay formation along the lower reaches of ephemeral rivers on the northern plains of arid central Australia. *Journal of Sedimentary Research* **75**: 636–649. https://doi.org/10.2110/jsr.2005.052.

Wentworth CK. 1922. A scale of grade and class terms for clastic sediments. *Journal of Geology* **30**: 377–392. https://doi.org/10.1086/521238.

Williams BPJ, McKie T. 2009. Preface: Triassic basins of the Central and North Atlantic Borderlands: models for exploration. *Geological Journal* **44**: 627–630.

Yuill BT, Khadka AK, Pereira J, Allison MA, Meselhe EA. 2016. Morphodynamics of the erosional phase of crevasse-splay evolution and implications for river sediment diversion function. *Geomorphology* **259**: 12–29. https://doi.org/10.1016/j.geomorph.2016.02.005.

Zwoliński Z. 1992. Sedimentology and geomorphology of overbank flows on meandering river floodplains. *Geomorphology* **4**: 367–379. https://doi.org/10.1016/0169-555X(92)90032-J.